2003

Activation Of Jnk By Vanadate Induces A Fas-Associated Death Domain (Fadd)-Dependent Death Of Cerebellar Granule Progenitors In Vitro

Jia Luo

Yanbo Sun

Hong Lin

Yong Qian

Zheng Li

See next page for additional authors

THE JOURNAL OF BIOLOGICAL CHEMISTRY Vol. 278, No. 7, Issue of February 14, pp. 4542–4551, 2003
Printed in U.S.A.

Activation of JNK by Vanadate Induces a Fas-associated Death Domain (FADD)-dependent Death of Cerebellar Granule Progenitors *in Vitro**

Received for publication, August 13, 2002, and in revised form, November 21, 2002
Published, JBC Papers in Press, November 25, 2002, DOI 10.1074/jbc.M208295200

Jia Luo‡§, Yanbo Sun‡, Hong Lin‡, Yong Qian¶, Zheng Li‡, Stephen S. Leonard¶, Chuanshu Huang‖, and Xianglin Shi¶

From the ‡Department of Microbiology, Immunology and Cell Biology, West Virginia University School of Medicine, Robert C. Byrd Health Science Center, Morgantown, West Virginia 26506, ¶Pathology and Physiology Research Branch, NIOSH, National Institutes of Health, Morgantown, West Virginia 26505, and ‖New York University Medical Center, Nelson Institute of Environmental Medicine, Tuxedo, New York 10987

Apoptosis is a highly regulated process that plays a critical role in neuronal development as well as the homeostasis of the adult nervous system. Vanadate, an environmental toxicant, causes developmental defects in the central nervous system. Here, we demonstrated that vanadate induced apoptosis in cultured cerebellar granule progenitors (CGPs). Treatment of cultured CGPs with vanadate activated ERKs and JNKs but not p38 MAPK and also induced c-Jun phosphorylation. In addition, vanadate induced FasL production, Fas (CD95) aggregation, and its association with the Fas-associated death domain (FADD), as well as the activation of caspase-8. Furthermore, vanadate generated reactive oxygen species (ROS) in CGPs; however, ROS was not involved in vanadate-mediated MAPK activation. Vanadate-induced FasL expression was ROS-dependent but JNK-independent. In contrast, vanadate-elicited Fas aggregation and Fas-FADD association, as well as caspase-8 activation, were dependent on JNK activation but were minimally regulated by ROS generation. The hydrogen peroxide scavenger, catalase, blocked vanadate-induced FasL expression and partially mitigated vanadate-induced cell death. On the other hand, dominant negative FADD and caspase-8 inhibitor completely eliminated vanadate-induced apoptosis. Thus, JNK signaling plays a major role in vanadate-mediated activation of the Fas-FADD-caspase-8 pathway that accounts for vanadate-induced apoptosis of CGPs.

Apoptosis, or programmed cell death, plays an important role in shaping the developing nervous system, removing unwanted neurons, and establishing correct synaptic connections with the targets they innervate (1–4). In the adult, inappropriate apoptosis in the central nervous system may contribute to a number of neurodegenerative diseases including Alzheimer's disease, Parkinson's disease, and stroke (5–8). Understanding the mechanisms that govern neuronal apoptosis could lead to more effective therapies for these disorders.

Mitogen-activated protein kinases (MAPKs)[1] play an instrumental role in the transmission of signals from cell surface receptors and environmental cues to the transcriptional machinery. Three major MAPKs have been identified: the extracellular signal-regulated kinases (ERKs), the c-Jun NH_2-terminal protein kinases (JNKs), and the p38 mitogen-activated protein kinase (p38 MAPK). ERKs are mainly activated by growth factors and are involved in the regulation of cell proliferation (9, 10). Unlike ERKs, JNKs and p38 MAPK are most potently activated by environmental stresses. JNKs are identified through their ability to phosphorylate the N-terminal stimulatory sites of c-Jun (11). Along with JNKs, p38 MAPKs are implicated in the regulation of cell death. JNKs and p38 MAPK may regulate apoptosis positively or negatively depending on cell type (12–15). However, the mechanisms by which JNKs and p38 MAPKs regulate neuronal apoptosis are not clear. Conflicting results have been published regarding the role of JNKs and p38 MAPK signaling in the control of neuronal apoptosis (16–26).

The trace metal vanadium is widely distributed in the environment (27, 28). It exists in oxidation states ranging from −1 to +5. Among these oxidation states the pentavalent state is the most stable form. In mammalian systems vanadium, the vanadate, is the most toxic form. Occupational exposure to vanadium is common in oil-fired electrical generating plants and petrochemical, steel, and mining industries (28, 29). Vanadate-containing compounds exert toxic effects on a wide variety of biological systems (30–34). Developmental exposure to vanadium is teratogenic and results in profound defects in the central nervous system (35–40). The objective of this study was to determine the mechanisms of vanadate-induced damages to the developing central nervous system and define the role of MAPKs in the regulation of neuronal apoptosis.

The developing cerebellum is one of the regions that is most susceptible to environmental insults, and vanadium compounds are deposited in the human cerebellum (41). Cerebellum granule neurons, the major cerebellar neuronal population, are generated in the proliferative external germinal layer of the cerebellum during the first 2–3 postnatal weeks in the rat (42, 43). During the early postnatal period, cells in the

* This work was supported by National Institutes of Health Grants AA12968 and CA90385 (to J. L.). The costs of publication of this article were defrayed in part by the payment of page charges. This article must therefore be hereby marked "*advertisement*" in accordance with 18 U.S.C. Section 1734 solely to indicate this fact.

§ To whom correspondence should be addressed. Tel.: 304-293-7208; Fax: 304-293-7823; E-mail: jluo@hsc.wvu.edu.

[1] The abbreviations used are: MAPK, mitogen-activated protein kinase; BrdUrd, 5-bromo-2′-deoxyuridine; CGPs, cerebellar granule progenitors; DISC, death-inducing signaling complex; ERK, extracellular signal-regulated kinase; FADD, Fas-associated death domain; DN-FADD, dominant negative FADD; FasL, Fas ligand; JNK, c-Jun NH_2-terminal kinase; MTT, 3-(4,5-dimethylthiazol-2-yl)-2,5-diphenyltetrazolium bromide; MEK, MAPK/ERK kinase; PBS, phosphate-buffered saline; PTP, protein tyrosine phosphatase; ROS, reactive oxygen species; ELISA, enzyme-linked immunosorbent assay; DMPO, 5,5-dimethyl-1-pyrroline *N*-oxide; DISC, death-inducing signal complex; APAF-1, apoptotic protease-activating factor-1.

external germinal layer undergo extensive proliferation to generate a large pool of cerebellar granule progenitors (CGPs). The developing CGPs then exit the cell cycle and migrate inward past Purkinje cell bodies to their final destination in the internal granule layer, where they differentiate into cerebellar granule neurons (42, 43). The CGPs isolated from 3–5-day (a time when CGPs are being generated and proliferating *in vivo*)-old rat pups retain their proliferative capability *in vitro* and are able to differentiate into neurons (44–47). This *in vitro* system offers an excellent model for study of neuronal development. Here, we demonstrate that vanadate induces apoptosis of CGPs. JNK signaling and the death receptor Fas (CD95) play a central role in vanadate-mediated neuronal death.

EXPERIMENTAL PROCEDURES

Reagents

Sodium metavanadate (vanadium (V), $NaVO_3$, or vanadate, catalog no. 2839-1) was purchased from Sigma. Caspase-3 inhibitor Ac-DMQD-CHO, caspase-8 inhibitor Z-IETD-FMK, and caspase-9 inhibitor ZlEHD-FMK were obtained from Calbiochem. Anti-Fas antibodies, SM1/23 and FL-335, were purchased from Alexis Biochemicals (San Diego, CA) and Santa Cruz Biotechnology (Santa Cruz, CA), respectively. Fas-Fc fusion protein was purchased from R&D Systems (Minneapolis, MN). Anti-Fas ligand (FasL) (N-20) and anti-FADD antibodies (H-181) were obtained from Santa Cruz Biotechnology. Human recombinant FasL was obtained from Upstate Biotechnology Inc. (Lake Placid, NY). Deferoxamine, superoxide dismutases, and sodium formate were purchased from Sigma. Catalase was obtained from Roche Molecular Biochemicals. The inhibitors for protein tyrosine phosphatase (α-bromo-4-hydroxyacetophenone), p38 MAPK (SB202190), and MEK1 (PD98059) were purchased from Calbiochem, and a selective JNK inhibitor (D-JNKI1) was purchased from Alexis Biochemicals.

Culture of CGPs

The CGPs were isolated from the cerebella of 3-day-old Sprague-Dawley rats (Hilltop Laboratory Inc., Scottsdale, PA) using a previously described procedure (47, 48). The purity of CGPs generated using this procedure is greater than 95.0%. Isolated CGPs were plated into poly-D-lysine (50.0 μg, Sigma)-coated culture wells or dishes at a density of $3.2 \times 10^4/cm^2$. The cultures were grown in Eagle's minimal essential medium containing the following supplements: 10.0% fetal bovine serum, 25.0 mM KCl, 1.0 mM glutamine, 33.0 mM glucose, and penicillin (100 units/ml)/streptomycin (100.0 μg/ml). Cells were incubated at 37 °C in a humidified environment containing 5.0% CO_2.

Cell Growth and Proliferation

The number of viable cells in culture was determined by the MTT assay (catalog no. 1 465 007, Roche Molecular Biochemicals). Briefly, the CGPs were plated into 96-well microtiter plates at a density of $3.2 \times 10^4/cm^2$. 10 μl of MTT labeling reagent was added to each well, and plates were incubated at 37 °C for 4 h. After MTT incubation the cultures were solubilized, and spectrophotometric absorbance of the samples was detected by a microtiter plate reader. The wavelength to measure the absorbance of formazan product was 570 nm with a reference wavelength of 750 nm. We have demonstrated that the MTT assay is an accurate method to determine the number of viable cells (47, 49). Cell proliferation was determined by pulse labeling of 5-bromo-2′-deoxyuridine (BrdUrd) (47, 50). Briefly, cells were plated into wells of removable chamber slides at the density of $3.2 \times 10^4/cm^2$ and exposed to 20.0 μM BrdUrd (Sigma) for 12 h. BrdUrd positive cells were visualized immunohistochemically using an anti-BrdUrd monoclonal antibody (Sigma). The numbers of BrdUrd positive and negative cells within an area of 0.5×0.5 mm were counted. Five fields were chosen at random in each slide and counted. A BrdUrd labeling index (the number of labeled cells divided by the total number of cells counted) was calculated.

Apoptosis Assays

Cellular DNA Fragmentation ELISA—This assay is based on quantification of accumulation of DNA fragments in the cytoplasm of apoptotic cells. Accumulation of cytosolic histone-bound DNA fragments was quantified using a commercial ELISA kit (catalog no. 1 544 675, Roche Molecular Biochemicals). The measurement of apoptosis, which was demonstrated previously, was sensitive, and the outcome was consistent with morphometric indices of apoptosis or the terminal deoxynucleotidyl transferase-mediated dUTP-biotin nick end-labeling assay (47, 51).

Nuclear Morphology—Cell death was also determined by counting the amount of cells containing condensed or fragmented nuclei in a blinded manner (52). Briefly, cells were fixed with 2.0% paraformaldehyde in phosphate-buffered saline (PBS) for 30 min at room temperature. Cell membranes were permeabilized by treating the cells with 0.10% Triton X-100 in PBS for 15 min and then stained with a DNA dye, TOTO-3 iodide (3.0 μg/ml; Molecular Probes Inc., Eugene, OR), for 30 min at 37 °C to visualize nuclear morphology. After being washed with PBS, the cells were examined under a Zeiss LSM 510 confocal microscope. Apoptotic neurons were determined by counting the cells containing condensed or fragmented nuclei in 4–5 fields/well. At least 200 cells were counted.

Caspase Activity

Caspase activity was determined using commercial fluorometric protease assay kits. Kits for assaying caspase-3 and caspase-8 activation were obtained from Santa Cruz Biotechnology and the caspase-9 activity kit from R&D Systems. The activation of caspases was determined for their protease activity by the addition of a caspase-specific substrate peptide that is conjugated to the fluorescent reporter molecule 7-amino-4-trifluoromethyl coumarin. The cleavage of the substrate peptide by specific caspase releases the fluorochrome that emits fluorescence at 505 nm when excited by light with a 400-nm wavelength. The level of caspase enzymatic activity is directly proportional to the fluorescence signal detected with a fluorometer.

Immunoblot and Immunoprecipitation Analysis

Cell lysates (40–100 μg of protein) were resolved by SDS-PAGE on 8–12% polyacrylamide gels, and separated proteins were transferred to nitrocellulose membranes. After blocking with 5.0% nonfat milk in TPBS (0.010 M PBS, pH 7.4, and 0.10% Tween 20) at room temperature for 1 h, the membranes were probed with various antibodies directed against activated MAPKs or phosphorylated tyrosine. These antibodies include anti-phospho-c-Jun, anti-phospho-p38 MAPK, anti-phospho ERK, anti-JNK1, anti-c-Jun, anti-p38, and anti-ERK, which were obtained from Santa Cruz Biotechnology. Anti-phospho-JNK antibody was purchased from Promega (Madison, WI) and anti-phosphotyrosine antibody from Cell Signaling Technology, Inc. (Beverly, MA). The antibody-antigen complexes were visualized by enhanced chemiluminescence (Amersham Biosciences). The blots were stripped and reprobed with an anti-β-actin antibody (Santa Cruz Biotechnology). The variation in loading was normalized against the amount of actin expression in each lane. Each experiment was repeated three to four times for each primary antibody. The relative amount of specific protein imaged on the films was quantified using a Sigma Gel program (Jandel, San Rafael, CA). Fas was immunoprecipitated from cell lysates (200.0 μg of total protein) by an anti-Fas antibody (Santa Cruz Biotechnology) using a previously described method (53). Immunoprecipitates were electrophoretically separated and transferred to nitrocellulose membranes. FADD associated with Fas was examined by immunoblotting using an anti-FADD antibody.

Fas Aggregation

Fas aggregation was determined using a previously described method (54, 55). Basically, when antibody is limiting (0.1–0.5 μg/ml), more molecules of the Fas will be immunoprecipitated if aggregation occurs after vanadate treatment. In contrast, when antibody is not limiting (5–10 μg/ml), equal amounts of Fas should be immunoprecipitated. Briefly, cells were treated with vanadate (25.0 μM, 6 h), resuspended in 500 μl of PBS, and then incubated with 2.0 mM cross-linker 3,3′-dithiobis-[sulfosuccinimidyl propionate] (Sigma) for 15 min on ice. The reaction was quenched with 10.0 mM ammonium acetate for 10 min and the cells were washed with PBS and then lysed. Fas was immunoprecipitated using either limiting or excess amounts of anti-Fas antibody and detected by immunoblot.

Cell Transfection

The pcDNA3.0/DN-FADD vector (kindly provided by Dr. V. M. Dixit, Genetech, San Francisco, CA) carries a truncated FADD cDNA lacking the death effector domain (DED) region (56, 57). pEGFP-C3 encoding the green fluorescent protein was obtained from Clontech Laboratories (Palo Alto, CA). The cells were transfected with pEGFP-C3 (0.30 μg) and DN-FADD (1.0 μg) or an empty pcDNA3.0 vector (1.0 μg) using LipofectAMINE 2000 reagent (Invitrogen) according to the manufacturer's instructions. One day after the transfection the CGPs were treated with vanadate (25.0 μM) for 24 h. Nuclei were stained with

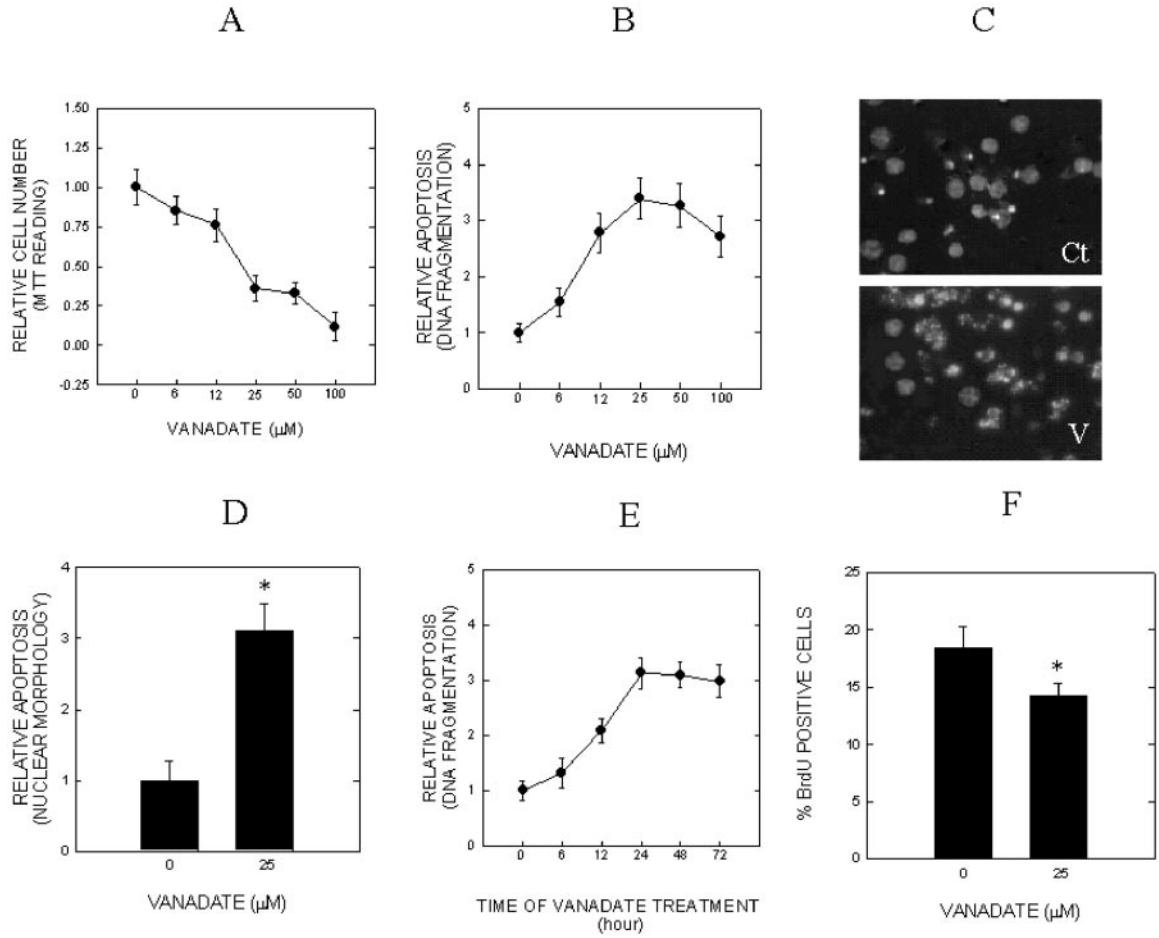

FIG. 1. **Effects of vanadate on the survival and proliferation of CGPs.** The CGPs were plated at a density of $3.2 \times 10^4/cm^2$. At 24 h after plating cells were treated with vanadate. *A*, effect of vanadate on cell number. Cells were exposed to vanadate (0–100.0 μM) for 48 h, and the number of viable cells was determined with the MTT assay. *B*, vanadate-induced apoptosis. Cells were exposed to vanadate (0–100.0 μM) for 24 h, and apoptosis was determined by a DNA fragmentation ELISA. *C*, assaying apoptosis by nuclear morphology. Cells were exposed to vanadate (25.0 μM) for 24 h and stained with the DNA dye TOTO-3 iodide (3.0 μg) for 30 min. Cells were examined under a confocal microscope. *D*, relative apoptosis shown in *C* was quantified by determining the nuclei fragmentation and condensation as described under "Experimental Procedures." *E*, time course of vanadate-mediated apoptosis. Cells were exposed to vanadate (25.0 μM) for various durations (6–72 h), and apoptosis was determined with a DNA fragmentation ELISA. *F*, DNA synthesis. Cells were treated with vanadate (25.0 μM) for 24 h. Subsequently, cells were exposed to BrdUrd (20.0 μM) for 12 h. The incorporation of BrdUrd was determined immunohistochemically as described under "Experimental Procedures." Each data point (*bars*; ± S.E.) is the mean of 3–4 independent trials. *, denotes a statistically significant difference between control and treated groups ($p < 0.05$).

TOTO-3 iodide, and apoptotic neurons in total transfected (green fluorescent protein-positive) cells were determined as described above.

Electron Spin Resonance (ESR) Measurements

The ESR spin trapping technique with 5,5-dimethyl-1-pyrroline *N*-oxide (DMPO) as the spin trap was used to detect free radical generation. This technique involves the formation of an adduct of a short-lived radical with a diamagnetic compound (spin trap) to generate a relatively long-lived free radical product (spin adduct), which can be studied by conventional ESR. The intensity of the spin adduct signal corresponds to the amount of short-lived radicals trapped, whereas the hyperfine couplings of the spin adduct are characteristics of trapped radicals. The spectra were recorded using a Varian E9 ESR spectrometer and a flat cell assembly as described previously (58). Hyperfine couplings were measured (to 0.1 G) directly from magnetic field separation using potassium tetraperoxochromate (K_3CrO_8) and 1,1-diphenyl-2-picrylhydrazyl as reference standards. 500.0 μl of cell suspension (1×10^6/0.5 ml) was mixed with 500.0 μl of PBS containing 100.0 mM DMPO and 1.0 mM vanadate with/without ROS scavengers. The reaction mixture (500.0 μl) was transferred to a flat cell for ESR measurement.

Statistical Analysis

Treatment groups were compared using analysis of variance. In cases where significant differences ($p < 0.05$) were detected, specific post hoc comparisons between treatment groups were examined with the Student-Newman-Keuls tests.

RESULTS

Vanadate-induced Apoptosis in Cultured CGPs—Vanadate exposure reduced the number of viable cells in a concentration-dependent manner (Fig. 1*A*). Concomitantly, vanadate increased apoptotic death, which was determined by a cellular DNA fragmentation ELISA in a dose-dependent manner (Fig. 1*B*). At a concentration of 25.0 μM, vanadate treatment (24 h) increased death rate by 3.4-fold. Vanadate-induced apoptosis was verified with an analysis of nuclear morphology by TO-TO-3 iodide staining; it showed a 3.1-fold increase in apoptotic rate after vanadate treatment (Fig. 1, *C* and *D*). Time course analysis revealed that maximal apoptosis occurred 24–48 h after vanadate treatment (Fig. 1*E*). Because CGPs proliferate in culture, we sought to determine whether vanadate affects the proliferation of CGPs. As shown in Fig. 1*F*, vanadate (25.0 μM) produced a small but statistically significant decrease (−19%; $p < 0.05$) of BrdUrd positive cells. In contrast, at this concentration vanadate decreased the number of CGPs by more than 70%. When these facts are taken together, it can be concluded that vanadate-induced depletion of cell number was mainly caused by the cell death.

Vanadate-mediated MAPK Activation—Vanadate produced

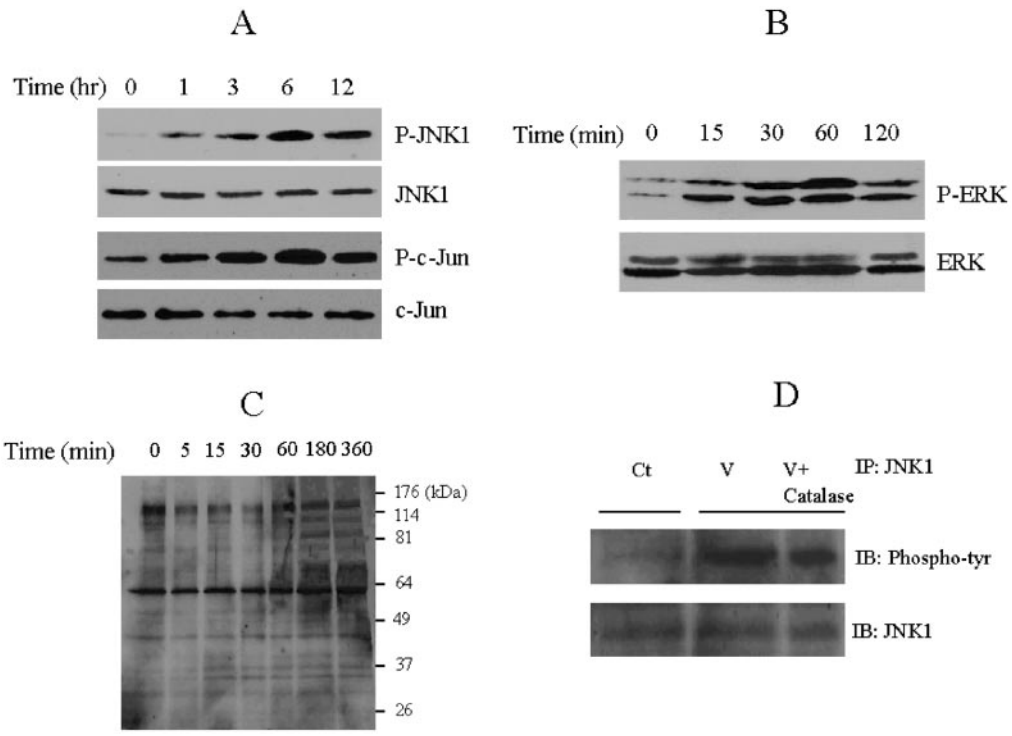

FIG. 2. **Vanadate-mediated activation of MAPK and protein tyrosine phosphorylation.** The CGPs were grown in a serum-free medium for 24 h and treated with vanadate (25.0 μM) for various lengths of time. The activation of MAPKs and protein tyrosine phosphorylation was determined with immunoblotting using specific antibodies. After detection of phosphorylated forms of MAPKs, the blots were stripped and reprobed with antibodies directed against nonphosphorylated kinases. *A*, JNK and c-Jun activation; *B*, ERK activation; *C*, protein tyrosine phosphorylation; *D*, tyrosine phosphorylation on JNK1. Cells were exposed to vanadate with/without catalase for 6 h, and JNK1 was immunoprecipitated using a specific antibody. The immunoprecipitates were assayed for tyrosine phosphorylation (*top panel*) or JNK1 expression (*bottom panel*). The experiments were replicated three times.

a sustained activation of JNK1 but did not affect JNK1 expression (Fig. 2*A*). The antibody applied reacts with both JNK1 and JNK2 (Promega, catalog no. V7932), but only phosporylated JNK1 was detected. The activation lasted for at least 12 h. As a result of JNK activation, vanadate induced phosphorylation of c-Jun, a main target of JNKs, in a pattern similar to that of JNK1 (Fig. 2*A*). Vanadate had little effect on c-Jun expression. Vanadate also produced a transient activation of ERK1/2 (Fig. 2*B*). The activation of ERK1/2 was evident 15 min after vanadate treatment, and the effect diminished after 2 h. Vanadate had little effect on the expression of ERK1/2. We also examined the effect of vanadate on p38 MAPK. Vanadate did not significantly alter either the expression or the activation of p38 MAPK in CGPs (data not shown). Vanadium compounds may serve as protein tyrosine phosphatase (PTP) inhibitor and subsequently enhance protein tyrosine phosphorylation (59, 60). We then examined the effect of vanadate on protein tyrosine phosphorylation of total cellular extracts. As shown in Fig. 2, *C* and *D*, vanadate treatment increased tyrosine phosphorylation on a number of proteins including JNK1 as determined by immunoprecipitation.

Vanadate-induced FasL Production, Fas-FADD Association, Fas Aggregation, and Caspase Activation—Because vanadate induced apoptotic death of CGPs (Fig. 1), we sought to determine the mechanisms of vanadate-induced damage. Death receptor Fas is an apoptotic sensor that transmits a death signal (61, 62). The adapter molecule FADD couples with the death receptor Fas to procaspase-8 (63). As shown in Fig. 3*A*, vanadate produced a concentration-dependent up-regulation in the expression of FasL. Although vanadate did not alter the expression of Fas and FADD, it induced an association between these proteins (Fig. 3*B*). Vanadate-induced activation of Fas was further confirmed by the evidence showing an increase in Fas aggregation (Fig. 3*C*). As shown in Fig. 3*C*, vanadate induced a JNK-dependent Fas aggregation. Because caspases play a critical role in the initiation of apoptosis, we sought to determine whether vanadate activates caspases. As shown in Fig. 4, vanadate treatment significantly ($p < 0.05$) activated caspases-3 and -8, but had little effect on caspase-9 (Fig. 4).

Vanadate-induced ROS Generation—ROS is involved in apoptosis (64). Vanadate is able to generate a whole spectrum of ROS, *i.e.* $O_2^{\cdot-}$, H_2O_2 and $^{\cdot}OH$ (65). To determine whether vanadate-induced apoptosis of CGPs is mediated by ROS, we first examined the ROS generation in the vanadate-treated cells. The ability of vanadate to generate $^{\cdot}OH$ radicals was examined using an ERS spin trapping method with DMPO as the spin trap. As shown in Fig. 5, vanadate treatment generated a typical ESR spectrum of free radicals. The spectrum consists of a 1:2:2:1 quartet with splittings of $a_H = a_N = 14.9$ G, where a_N and a_H denote hyperfine splitting of the nitroxyl nitrogen and α–hydrogen, respectively. On the basis of these splittings and the 1:2:2:1 line shape, this spectrum was assigned to the DMPO/$^{\cdot}OH$ adduct, which is evidence for $^{\cdot}OH$ radical generation. The addition of catalase, a specific H_2O_2 scavenger, completely eliminated the $^{\cdot}OH$ radical, indicating that H_2O_2 was generated in vanadate-stimulated cells and was a precursor of $^{\cdot}OH$ generation. Sodium formate, a scavenger of $^{\cdot}OH$ radical, and deferoxamine, a metal chelator, decreased the intensity of the radical signal. In contrast, superoxide dismutase, an $O_2^{\cdot-}$ scavenger the function of which is to convert $O_2^{\cdot-}$ to H_2O_2, increased the DMPO/$^{\cdot}OH$ adduct signal. The results were similar in three independent experiments. The finding indicated that vanadate was able to generate a whole spectrum of ROS in CGPs.

Vanadate-induced FasL Production and Fas-FADD Association Involve Different Mechanisms—Catalase, a specific H_2O_2 scavenger, eliminated vanadate-induced ROS generation (Fig.

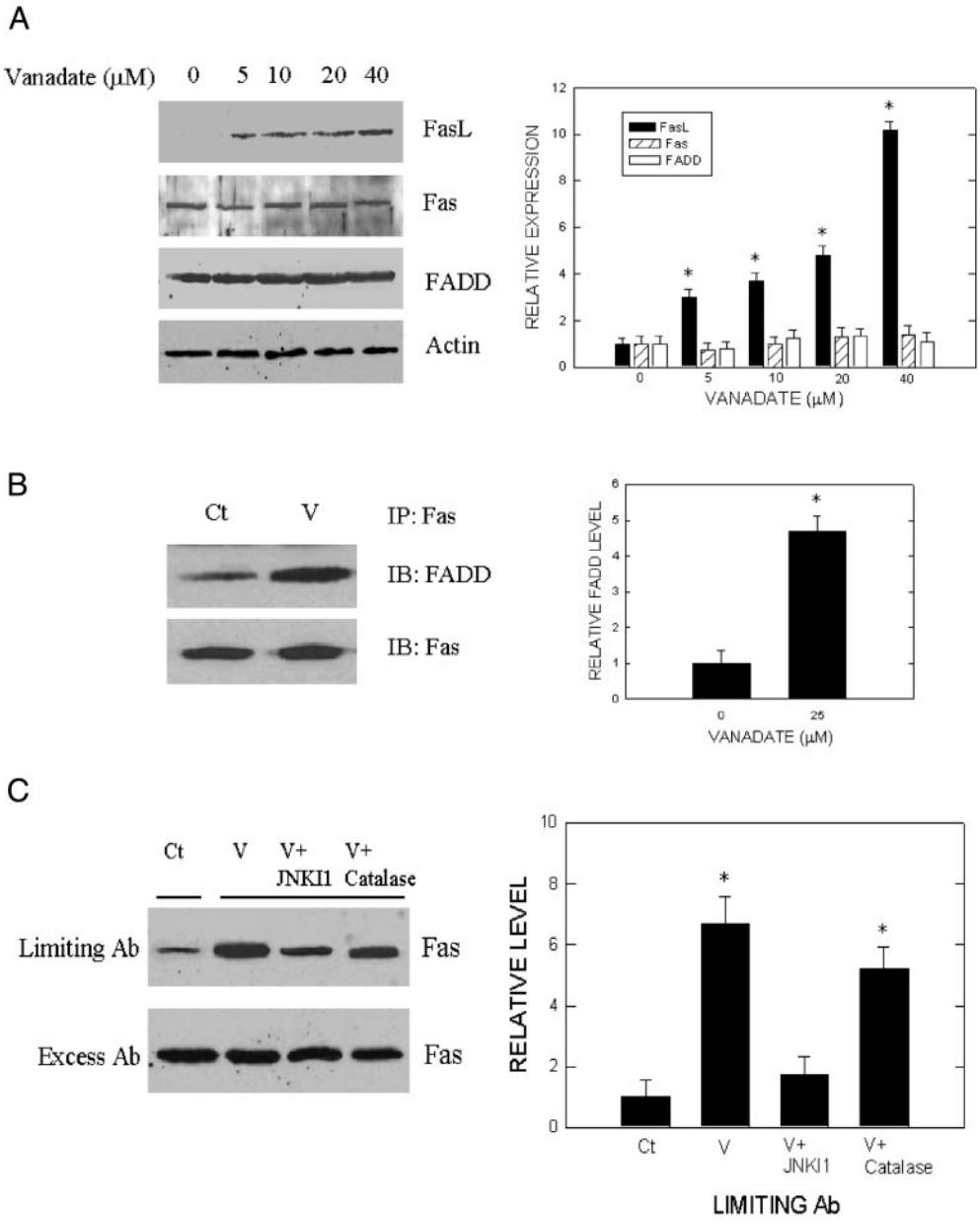

FIG. 3. **Effects of vanadate on FasL, Fas, and FADD.** *A*, expression of FasL, Fas, and FADD. The CGPs were treated with vanadate (0–40.0 μM) for 24 h, and total proteins were isolated. Equal amounts of proteins (60.0 μg) were subjected to immunoblot analysis. After the detection of FasL, Fas, and FADD, the blots were stripped and reprobed with an anti-actin antibody. *B*, vanadate-mediated association between Fas and FADD. Cells were treated with vanadate (25.0 μM) for 6 h, and proteins were isolated. Cell lysates were immunoprecipitated with an anti-Fas antibody and probed with an anti-FADD antibody. *C*, vanadate-mediated Fas aggregation. Cells were treated with vanadate (25.0 μM) for 6 h in the presence/absence of D-JNKI1 or catalase. Cell lysates were treated with a cross-linking reagent and immunoprecipitated using an anti-Fas antibody under antibody-limiting conditions (*top panel*) or antibody-excess conditions (*bottom panel*). Panels on the *right* were the microdensitometrical quantification of relative expression. Each data point (*bars*; ± S.E.) is the mean of three independent trials. *, denotes a statistically significant difference between control and treated groups ($p < 0.05$).

5); however, it did not affect vanadate-mediated JNK and ERK activation (Figs. 2*D* and 6). D-JNKI1, a specific inhibitor for JNK1/2 (66), and PD98059, an inhibitor for MEK1, completely blocked vanadate-induced phosphorylation of c-Jun and ERK1/2, respectively. Interestingly, although catalase did not block vanadate-induced MAPK activation, it eliminated the vanadate-mediated increase in FasL production (Fig. 7*A*). In contrast, D-JNKI1 and other ROS scavengers/promoters did not significantly alter FasL production (Fig. 7*A*). The levels of FasL were also unaffected by PD98059 (data not shown). These results indicated that the H_2O_2 was critical in vanadate-induced increase in FasL expression.

Because catalase blocked the vanadate-induced increase in FasL expression, we examined the effect of catalase on Fas aggregation and Fas-FADD association. As shown in Figs. 3*C* and 7*B*, catalase produced a modest inhibition on vanadate-induced Fas aggregation and Fas-FADD association. Despite its lack of effect on FasL production, D-JNKI1 dramatically inhibited vanadate-induced Fas aggregation and Fas-FADD association. The combination of catalase and D-JNKI1 treatment completely abolished vanadate-mediated Fas-FADD association (Fig. 7*B*). PD98059 did not affect the interaction between Fas and FADD. Taken together, these observations indicate that vanadate-induced FasL production is independent of MAPK activation but is dependent on H_2O_2 generation. In contrast, JNK activation is not required for vanadate-in-

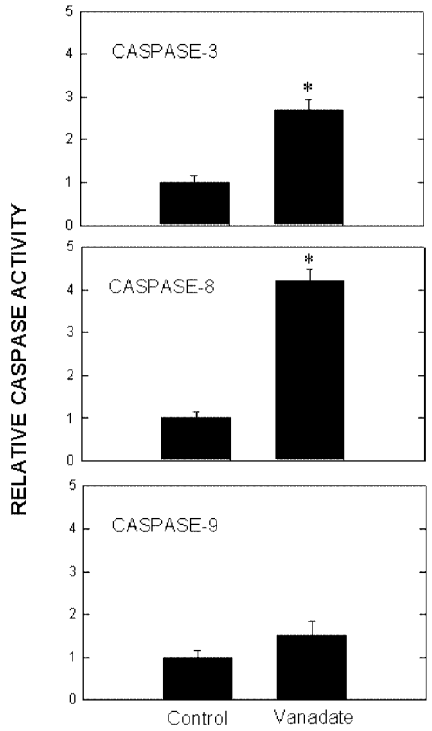

FIG. 4. **Effects of vanadate on caspase activity.** The CGPs were treated with vanadate (25.0 μM) for 24 h. The activity of caspase-3, -8, and -9 was determined as described under "Experimental Procedures." Each data point (*bars*; ± S.E.) is the mean of four independent trials. *, denotes a statistically significant difference between control and treated groups ($p < 0.05$).

duced increase in FasL production but is essential for the activation of Fas and subsequent Fas-FADD association.

Because vanadate-induced JNK activation triggered Fas-FADD association, we further examined whether the activation of caspase-8 was mediated by JNKs. As shown in Fig. 7*C*, D-JNKI1 abolished vanadate-induced caspase-8 activation. On the other hand, catalase produced only a marginal inhibition on vanadate-induced caspase-8 activation. PD98059 had no effect on caspase-8 activation.

Vanadate-induced Apoptosis Is Mediated by FADD-Caspase-8 Pathway—Because vanadate increased FasL expression (Fig. 3*A*), we sought to determine whether the apoptosis of CGPs is mediated by the FasL-Fas interaction. Two Fas antagonists, SM1/23 and Fas-Fc, were introduced. These antagonists effectively abolished FasL-Fas interaction (67, 68) and eliminated recombinant FasL-induced apoptosis in CGPs (data not shown). However, both antagonists produced only a modest but statistically significant ($p < 0.05$) inhibition of vanadate-induced apoptosis (Fig. 8). These results suggested that although FasL induction was involved it was not the primary mechanism for vanadate-induced apoptosis of CGPs.

The Fas-mediated apoptotic pathway is initiated by the recruitment of FADD followed by the cleavage and activation of caspase-8 (61). To examine whether vanadate-induced cell death is mediated by the FADD-caspase-8 pathway, we used DN-FADD and the caspase-8 inhibitor, Z-IETD-FMK, to block the action of FADD and caspase-8, respectively. As shown in Fig. 9, both DN-FADD and Z-IETD-FMK eliminated vanadate-induced cell death. Blockage of the activation of caspase-3 but not caspase-9 also significantly inhibited vanadate-induced apoptosis (Fig. 9*B*). These results support the notion that the Fas-FADD-caspase-8 pathway plays a major role in vanadate-triggered cell death in CGPs.

To further investigate the role of JNK activation and ROS in vanadate-induced apoptosis, we determined whether blockage of MAPK activation or H_2O_2 removal could protect CGPs from vanadate-induced cell death. Removal of H_2O_2 by catalase produced a partial and statistically significant ($p < 0.05$) rescue (Fig. 10). Inhibition of JNK activation exerted a more potent protection against vanadate-induced damage. Furthermore, simultaneous treatment with catalase and D-JNKI1 completely abolished vanadate-mediated cell death. Vanadate-triggered cell death remained unaffected by both PD98059 and SB 292190 treatment.

Vanadate may serve as a PTP inhibitor. To determine whether other inhibitors for PTP have the same effect as vanadate, we examined the effect of α-bromo-4-hydroxyacetophenone, a specific PTP inhibitor, on CGPs. The results indicated that this inhibitor did not significantly induce apoptosis (data not shown), suggesting that the effect of vanadate is not mediated by a general inhibition of tyrosine dephosphorylation.

DISCUSSION

The present study demonstrates that vanadate at physiologically relevant concentrations (10–100 μM) inhibits the growth of cultured CGPs. These concentrations, which range in micromoles, are comparable with the levels encountered in industrial settings (29). The CGPs proliferate *in vitro,* and vanadate produces a marginal inhibition of the proliferation of CGPs. On the other hand, vanadate dramatically increases the death of CGPs. Therefore, vanadate-induced growth inhibition mainly results from cell death. Vanadate-induced death of CGPs is typical of apoptosis, which is verified by measuring various apoptotic indices. Furthermore, the present study characterizes a signaling pathway that explains how vanadate exposure induces neuronal apoptosis.

In general, the apoptotic signal can be transmitted through either the death receptors, such as Fas, or mitochondria (63). Fas (also called APO-1 or CD95) is a member of the tumor necrosis receptor superfamily that transmits a death signal to the cells (61). In Fas-mediated death, it is well known that the binding to its ligand, FasL, or agonist antibodies induces aggregation of the receptor, which results in its interaction with the death adapter molecule Fas-associated death domain (FADD, also called MORT1) (63). FADD contains a death domain (DD) and a death effector domain (DED). On activation, Fas associates with the death domain in FADD (61). Subsequently, procaspase-8 binds to the DED of FADD and forms a death-inducing signal complex (DISC). on forming a DISC, procaspase-8 is activated autoproteolytically and propagates the apoptotic signal by activating executioner caspases such as caspase-3 (63, 69, 70). Formation of the DISC could be FasL-dependent or independent (51–74). In mitochondria-mediated cell death, mitochondria sense the apoptotic signal and convey it to the activation of adapter APAF-1 via the release of cytochrome *c*. Cytochrome *c* binds to APAF-1, and in the presence of adenine nucleotides the APAF-1-cytochrome *c* complex promotes activation of procaspase-9 (75). Caspase-9 can activate executioner caspases and trigger apoptosis (63).

Vanadate clearly triggers a death signal mediated by the death receptor Fas. It up-regulates FasL expression, promotes the Fas aggregation and the association of Fas with FADD, and subsequently activates caspases (caspase-8 and -3). Apparently, vanadate-induced apoptosis occurs through this pathway because blocking this pathway by either a DN-FADD or caspase-8 inhibitor eliminates vanadate-induced cell death. In Fas-mediated apoptosis, Fas is activated first by the binding to its ligand (FasL) or agonist antibody (61). Our results show that vanadate induces a robust increase of FasL expression. Surprisingly, it appears that the FasL induction has a relatively minor contribution to vanadate-induced apoptosis. This

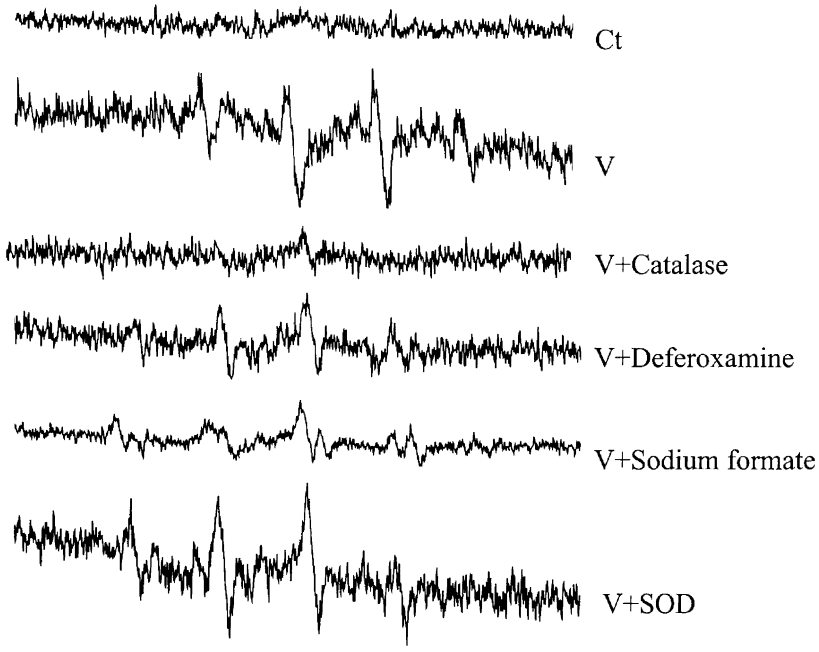

FIG. 5. **Measurement of vanadate-induced ROS generation by ESR.** The CGPs (1×10^6) were incubated in PBS containing 100.0 mM DMPO and 1.0 mM vanadate with or without different ROS scavengers as indicated. ESR spectra were recorded for 30 min. The final concentrations for ROS scavengers were: catalase, 2000 units/ml; superoxide dismutase, 5.0 μg/ml; formate, 50.0 mM; and deferoxamine, 2.0 mM.

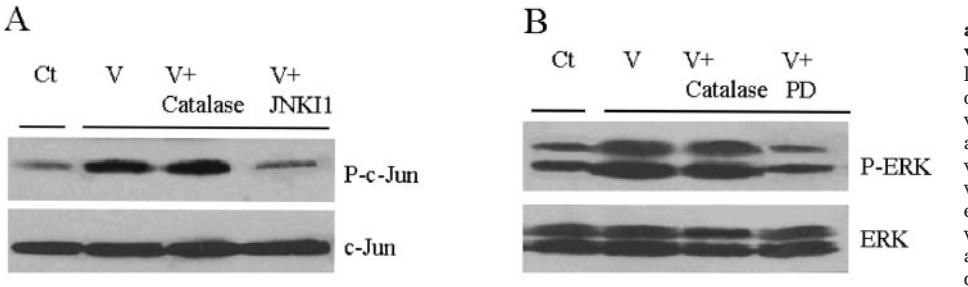

FIG. 6. **Effects of catalase, D-JNKI1, and PD98059 on c-Jun and ERK activation.** Cells were pretreated with catalase (2000 units/ml), PD98059 (50.0 μM), or D-JNKI1 (1.0 μM) for 30 min before vanadate treatment (25.0 μM). *A*, c-Jun activation. Cells were then exposed to vanadate for 6 h, and c-Jun activation was determined as described in the legend for Fig. 2. *B*, ERK activation. Cells were then exposed to vanadate for 30 min, and ERK activation was determined as described in the legend for Fig. 2.

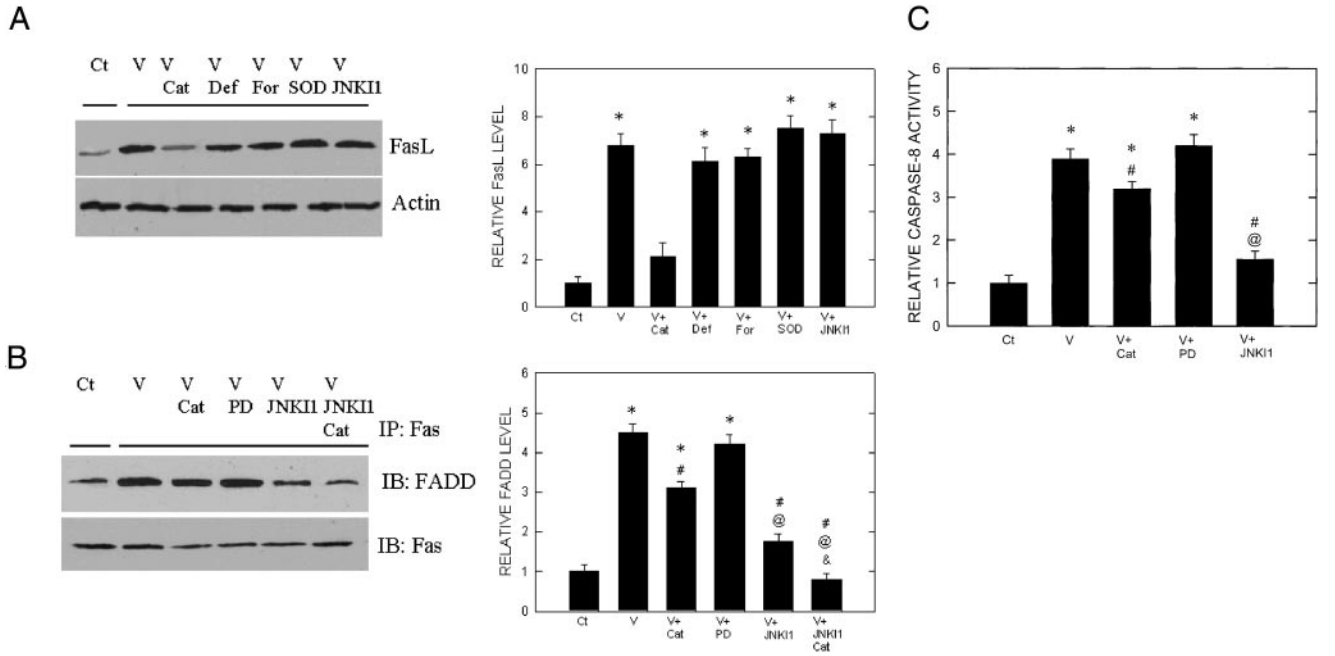

FIG. 7. **Effects of ROS scavengers and inhibitors for MAPKs on vanadate-induced FasL production, Fas-FADD association, and caspase-8 activation.** Cells were pretreated with catalase (2000 units/ml), PD98059 (50.0 μM), or D-JNKI1 (1.0 μM) for 30 min before vanadate treatment (25.0 μM). *A*, FasL expression. Cells were exposed to vanadate for 24 h, and the expression of FasL was determined by immunoblot. *B*, Fas-FADD association. Cells were then exposed to vanadate for 6 h, and Fas-FADD association was determined as described in Fig. 3. Panels on the *right* were the microdensitometrical quantification of relative expression. *C*, caspase-8 activation. Cells were exposed to vanadate for 24 h, and the activation of caspase-8 was determined as described under "Experimental Procedures." The experiments were replicated three to four times. *, statistically significant difference relative to control cultures ($p < 0.05$); #, statistically significant difference relative to vanadate-treated cultures ($p < 0.05$); @, statistically significant difference relative to vanadate- and catalase-treated cultures ($p < 0.05$); &, statistically significant difference relative to vanadate and JNKI-treated cultures ($p < 0.05$).

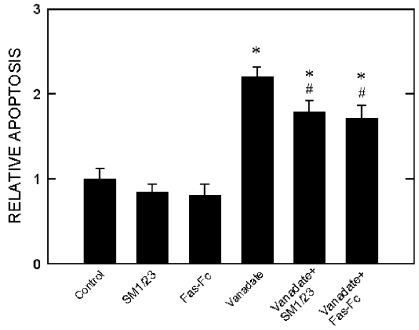

FIG. 8. **Effects of Fas antagonists on vanadate-mediated apoptosis.** CGPs were exposed to vanadate for 24 h with or without antibody SM1/23 (3.0 μg/ml) or Fas-Fc fusion protein (40.0 μM). Apoptosis was determined with a DNA fragmentation ELISA. The experiment was replicated four times. *, statistically significant difference relative to control cultures ($p < 0.05$); #, statistically significant difference relative to vanadate-treated cultures ($p < 0.05$).

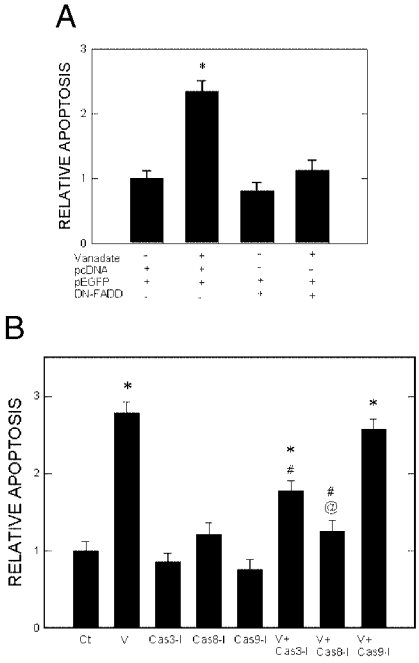

FIG. 9. **Effects of dominant negative FADD (*DN-FADD*) and caspase inhibitors on vanadate-mediated apoptosis.** *A*, cells were transfected with pEGFP-C3 and DN-FADD or empty pcDNA3.0 vector. One day after transfection cells were exposed to vanadate (25.0 μM) for 24 h, and apoptosis in the transfected cells was assayed by nuclei fragmentation and condensation after TOTO-3 iodide staining as described under "Experimental Procedures." Relative apoptosis in the total transfected cells (green fluorescent protein-positive) was quantified. *B*, cells were pretreated with different caspase inhibitors for 30 min before vanadate exposure (25.0 μM, 24 h). After vanadate treatment, apoptosis was determined with a DNA fragmentation ELISA. The inhibitors for caspase-3 (*Cas3-I*), caspase-8 (*Cas8-I*), and caspase-9 (*Cas9-I*) were Ac-DMQD-CHO, Z-IETD-FMK, and ZlEHD-FMK, respectively. Each data point (*bars*; ± S.E.) is the mean of three to four independent trials. *, denotes a statistically significant difference relative to control group ($p < 0.05$). #, statistically significant difference relative to vanadate-treated cultures ($p < 0.05$); @, statistically significant difference relative to vanadate and caspase 3-I-treated cultures ($p < 0.05$).

argument is based on the observations that (*a*) the elimination of vanadate-induced increase in FasL expression (by treatment of catalase) does not inhibit Fas-FADD association, and only produces a modest protection against vanadate-induced apoptosis, and (*b*) a blockage of FasL-Fas interaction by Fas antagonists has a marginal effect on vanadate-induced cell death. Thus, it can be concluded that, although it participates, FasL

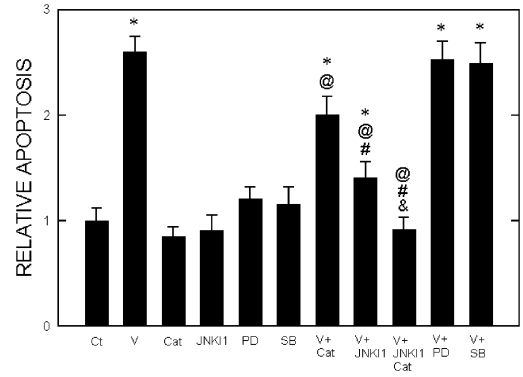

FIG. 10. **Effects of inhibitors for MAPKs and catalase on vanadate-induced apoptosis.** Cells were pretreated with catalase (2000 units/ml), PD98059 (50.0 μM), SB292190 (10.0 μM), or D-JNKI1 (1.0 μM) for 30 min before vanadate treatment (25.0 μM; 24 h). After vanadate exposure, apoptosis was determined with a DNA fragmentation ELISA. Each data point (*bars*; ± S.E.) is the mean of four independent trials. *, statistically significant difference relative to control cultures ($p < 0.05$); @, statistically significant difference relative to vanadate-treated cultures ($p < 0.05$); #, statistically significant difference relative to vanadate- and catalase-treated cultures ($p < 0.05$); *&*, statistically significant difference relative to vanadate- and JNKI1-treated cultures ($p < 0.05$).

induction is not the major contributor to vanadate-induced apoptosis. This may be the result of the inefficiency in the level of FasL induction to cause a substantial cell death. Therefore, there must be other mechanisms independent of FasL induction that account for vanadate-induced death of CGPs.

Vanadate activates two MAPKs, ERK1/2 and JNK1, in CGPs. The pattern of activation for each is different. The activation of ERKs is rapid and transient, whereas JNK activation is relatively slow and more persistent (lasting for at least 12 h). In addition, vanadate induces ROS generation in CGPs. It appears that H_2O_2 is the major precursor of the $^{\cdot}OH$ radical induced by vanadate because catalase (a specific H_2O_2 scavenger) eliminates the $^{\cdot}OH$ radical generated by vanadate. It has been demonstrated that many effects of vanadate are mediated by its ability to generate ROS. For example, vanadate-induced activation of transcription factors such as NF-κB, p53, or hypoxia-inducible factor 1α (HIF-1α) and the up-regulation of tumor necrosis factor α (TNFα) expression are clearly mediated by ROS generation, particularly through the H_2O_2 accumulation (76–79). Vanadate-induced JNK activation has been observed in mouse macrophages, and the activation is also dependent on ROS induction (76). However, the present study demonstrates that the H_2O_2 scavenger catalase does not affect the activation of JNK and ERKs, suggesting that ROS is not involved in vanadate-induced activation of MAPKs in CGPs. Vanadium compounds may serve as a PTP inhibitor that enhances protein tyrosine phosphorylation (59, 60). Our results show that vanadate increases tyrosine phosphorylation on JNK1, which suggests that vanadate-induced activation of signaling proteins is mediated by its inhibition of PTPs. Thus, it appears that the biological effect of vanadate is cell type-specific.

JNK activation can result in FasL expression in various cells (22, 80–82). However, the present study shows that neither JNK nor ERK activation is required for vanadate-induced increase in FasL production in CGPs. On the other hand, ROS appears to be indispensable for vanadate-induced FasL production; the H_2O_2 scavenger catalase completely blocks vanadate-induced FasL expression. The exact signal pathway underlying ROS regulation of FasL expression in CGPs remains to be elucidated. Although JNK activation is not involved in FasL induction, it is required for vanadate-induced Fas-FADD association. That is, vanadate-induced JNK activation initiates the

Fas-FADD-caspase pathway in a FasL-independent manner. This effect is mediated by FasL-independent Fas aggregation. It has been reported that JNK activation triggers FasL-independent aggregation of Fas and subsequently evokes the FADD-caspase pathway in Jurkat T cells (73). FasL-independent Fas aggregation has been observed on various stress stimuli, such as exposure to UV, cycloheximide, cisplatin, etoposide, vinblastine, curcumin, and doxorubicin (83–87).

Persistent activation of JNK is capable of triggering apoptotic pathways initiated by both the death receptor (such as Fas) and mitochondria (88). Apoptosis of CGPs caused by vanadate-induced JNK activation is mediated primarily by the death receptor Fas. This conclusion is supported by the following observations. First, vanadate-induced apoptosis is mediated by the FADD-caspase-8 pathway, and the blockage of JNK activation abolishes Fas-FADD association and caspase-8 activation. Second, inhibition of JNK activation significantly reduces vanadate-mediated cell death. FasL induction has a modest but statistically significant contribution to vanadate-induced apoptosis. Simultaneously blocking JNK activation and FasL expression totally abolishes vanadate-induced Fas-FADD association and the subsequent apoptosis. This result indicates that both JNK activation and FasL induction contribute to vanadate-induced apoptosis, and JNKs are the major contributors. Third, vanadate activates caspase-8 and -3 but not caspase-9. Fas activation (Fas aggregation) results in the formation of DISC that activates procaspase-8 (61). Activated caspase-8 directly cleaves procaspase-3, an executioner caspase, and triggers apoptosis (89). On the other hand, the activation of caspase-9 is triggered mainly by damage to mitochondria and the release of cytochrome *c*. It is noted, however, that cross-talk may exist between death receptor- and mitochondria-mediated cell death (90, 91).

In summary, JNK activation by vanadate initiates the Fas-FADD-caspase-8 signal pathway and triggers apoptosis in CGPs. The finding that vanadate induces apoptosis in central nervous system neurons may explain some of the central nervous system defects attributed to environmental exposure to vanadate. The JNK and FADD-caspase-8 signal pathways may also contribute to the neurotoxicity of other environmental toxicants, such as heavy metals. Like vanadate, the heavy metals, including arsenite, lead, lithium, and mercury, have been shown to induce neuronal apoptosis (26, 71, 92–93). Understanding the role of JNK in apoptosis of neuronal precursors will help elucidate the mechanisms of programmed cell death in the developing nervous system.

Acknowledgment—We thank Kimberly A. Bower for her reading of this manuscript.

REFERENCES

1. Cowan, W. M., Fawcett, J. W., O'Leary, D. D., and Stanfield, B. B. (1984) *Science* **225,** 1258–1265
2. Oppenheim, R. W. (1991) *Annu. Rev. Neurosci.* **14,** 453–501
3. Raff, M. C., Barres, B. A., Burne, J. F., Coles, H. S., Ishizaki, Y., and Jacobson, M. D. (1993) *Science* **262,** 695–700
4. Oppenheim, R. W., Prevette, D., D'Costa, A., Wang, S., Houenou, L. J., and McIntosh, J. M. (2000) *J. Neurosci.* **20,** 6117–6124
5. Gordon, N. (1995) *Brain Dev.* **17,** 73–77
6. Thompson, C. B. (1995) *Science* **267,** 1456–1462
7. Stefanis, L., Burke, R. E., and Greene, L. A. (1997) *Curr. Opin. Neurol.* **10,** 299–305
8. Honig, L. S., and Rosenberg, R. N. (2000) *Am. J. Med.* **108,** 317–330
9. Marshall, C. J. (1995) *Cell* **80,** 179–185
10. Blanchard, D. A., Mouhamad, S., Auffredou, M. T., Pesty, A., Bertoglio, J., Leca, G., and Vazquez, A. (2000) *Oncogene* **19,** 4184–4189
11. Hibi, M., Lin, A., Smeal, T., Minden, A., and Karin, M. (1993) *Genes Dev.* **7,** 2135–2148
12. Kummer, J. L., Rao, P. K., and Heidenreich, K. A. (1997) *J. Biol. Chem.* **272,** 20490–20494
13. Wang, X., Martindale, J. L., Liu Y., and Holbrook, N. J. (1998) *Biochem. J.* **333,** 291–300
14. Kimura, N., Matsuo, R., Shibuya, H., Nakashima, K., and Taga, T. (2000) *J. Biol. Chem.* **275,** 17647–17652
15. Schrantz, N., Bourgeade, M. F., Mouhamad, S., Leca, G., Sharma, S., and Vazquez, A. (2001) *Mol. Biol. Cell* **12,** 3139–3151
16. Kawasaki, H., Morooka, T., Shimohama, S., Kimura, J., Hirano, T., Gotoh, Y., and Nishida, E. (1997) *J. Biol. Chem.* **272,** 18518–18521
17. Yang, D. D., Kuan, C. Y., Whitmarsh, A. J., Rincon, M., Zheng, T. S., Davis, R. J., Rakic, P., and Flavell, R. A. (1997) *Nature* **389,** 865–870
18. Bazenet, C. E., Mota, M. A., and Rubin, L. L. (1998) *Proc. Natl. Acad. Sci. U. S. A.* **95,** 3984–3989
19. Kuan, C. Y., Yang, D. D., Samanta Roy, D. R., Davis, R. J., Rakic, P., and Flavell, R. A. (1999) *Neuron* **22,** 667–676
20. Luo Y., Umegaki H., Wang X., Abe, R., and Roth, G. S. (1998) *J. Biol. Chem.* **273,** 3756–3764
21. Behrens, M. M., Strasser, U., Koh, J. Y., Gwag, B. J., and Choi, D. W. (1999) *Neuroscience* **94,** 917–927
22. Le-Niculescu, H., Bonfoco, E., Kasuya, Y., Claret, F. X., Green, D. R., and Karin, M. (1999) *Mol. Cell. Biol.* **19,** 751–763
23. Mao, Z., Bonni, A., Xia, F., Nadal-Vicens, M., and Greenberg, M. E. (1999) *Science* **286,** 785–790
24. Camandola, S., Poli G., and Mattson, M. P. (2000) *J. Neurochem.* **74,** 159–168
25. Kanamoto, T., Mota, M., Takeda, K., Rubin, L. L., Miyazono, K., Ichijo, H., and Bazenet, C. E. (2000) *Mol. Cell. Biol.* **20,** 196–204
26. Namgung, U., and Xia, Z. (2000) *J. Neurosci.* **20,** 6442–6451
27. Boyd, D. W., and Kustin, K. (1984) *Adv. Inorg. Biochem.* **6,** 311–365
28. Nriagu, J. O., and Pacyna, J. M. (1988) *Nature* **333,** 134–139
29. Woodin, M. A., Liu, Y., Neuberg, D., Hauser, R., Smith, T. J., and Christiani, D. C. (2000) *Am. J. Ind. Med.* **37,** 353–363
30. Erdmann, E., Werdan, K., Krawietz, W., Schmitz, W., and Scholz, H. (1984) *Biochem. Pharmacol.* **33,** 945–950
31. Younes, M., Kayser, E., and Strubelt, O. (1991) *Toxicology* **70,** 141–149
32. Cohen, M. D., Klein, C. B., and Costa, M. (1992) *Mutat. Res.* **269,** 141–148
33. Stern, A., Yin, X., Tsang, S. S., Davison, A., and Moon, J. (1993) *Biochem. Cell Biol.* **71,** 103–112
34. Leonard, A., and Gerber, G. B. (1994) *Mutat. Res.* **317,** 81–88
35. Catalan, R. E., Martinez, A. M., Aragones, M. D., Robles, A., and Miguel, B. G. (1987) *Life Sci.* **40,** 799–806
36. Domingo, J. L. (1996) *Reprod. Toxicol.* **10,** 175–182
37. Figiel, I., and Kaczmarek, L. (1997) *NeuroReport* **8,** 2465–2470
38. Cardozo, J. (1998) *Invest. Clin.* **39,** Suppl. 1, 49–53
39. Faria de Rodriguez, C., Villalobos, H., and Nava de Leal, C. (1998) *Invest. Clin.* **39**, Suppl. 1, 55–85
40. Mandell, J. W., and Banker, G. A. (1998) *J. Neurobiol.* **35,** 17–28
41. Yukawa, M., Amano, K., Suzuki-Yasumoto, M., and Terai, M. (1980) *Arch. Environ. Health* **35,** 36–44
42. Miale, I. L., and Sidman, R. L. (1961) *Exp. Neurol.* **4,** 277–296
43. Altman, J. (1972) *J. Comp. Neurol.* **145,** 353–397
44. Cui, H., and Bulleit, R. F. (1998) *Dev. Brain Res.* **106,** 129–135
45. Wechsler-Reya, R. J., and Scott, M. P. (1999) *Neuron* **22,** 103–114
46. Miyazawa, K., Himi, T., Garcia, V., Yamagishi, H., Sato, S., and Ishizaki, Y. (2000) *J. Neurosci.* **20,** 5756–5763
47. Li, Z., Lin, H., Zhu, Y., Wang, M., and Luo, J. (2001) *Brain Res. Dev. Brain Res.* **132,** 47–58
48. Luo, J. West, J. R., and Pantazis, N. J. (1997) *Alcohol. Clin. Exp. Res.* **21,** 1108–1120
49. Sun, Y., Lin, H., Zhu, Y., Ma, C., Ye, J., and Luo, J. (2002) *J. Cell. Physiol.* **192,** 225–233
50. Luo, J., and Miller, M. W. (1997) *Brain Res.* **770,** 139–150
51. Ye, J., Ding, M., Leonard, S. S., Robinson, V. A., Millecchia, L., Zhang, X., Castranova, V., Vallyathan, V., and Shi, X. (1999) *Mol. Cell. Biochem.* **202,** 9–17
52. Morishima, Y., Gotoh, Y., Zieg, J., Barrett, T., Takano, H., Flavell, R., Davis, R. J., Shirasaki, Y., and Greenberg, M. E. (2001) *J. Neurosci.* **21,** 7551–7560
53. Luo, J., and Miller, M. W. (1999) *J. Neurosci.* **19,** 10014–10025
54. Rehemtulla, A., Hamilton, C. A., Chinnaiyan, A. M., and Dixit, V. M. (1997) *J. Biol. Chem.* **272,** 25783–25786
55. Ruiz-Ruiz, C., Robledo, G., Font, J., Izquierdo, M., and Lopez-Rivas, A. (1999) *J. Immunol.* **163,** 4737–4746
56. Chinnaiyan, A. M., O'Rourke, K., Tewari, M., and Dixit, V. M. (1995) *Cell* **81,** 505–512
57. Chinnaiyan, A. M., Tepper, C. G., Seldin, M. F., O'Rourke, K., Kischkel, F. C., Hellbardt, S., Krammer, P. H., Peter, M. E., and Dixit, V. M. (1996) *J. Biol. Chem.* **271,** 4961–4965
58. Shi, X. L., and Dalal, N. S. (1991) *Arch. Biochem. Biophys.* **289,** 355–361
59. Krejsa, C. M., Nadler, S. G., Esselstyn, J. M., Kavanagh, T. J., Ledbetter, J. A., and Schieven, G. L. (1997) *J. Biol. Chem.* **272,** 11541–11549
60. Barbeau, B., Bernier, R., Dumais, N., Briand, G., Olivier, M., Faure, R., Posner, B. I., and Tremblay, M. (1997) *J. Biol. Chem.* **272,** 12968–12977
61. Nagata, S. (1997) *Cell* **88,** 355–365
62. Nagata, S. (1999) *Annu. Rev. Genet.* **33,** 29–55
63. Wolf, B. B., and Green D. R. (1999) *J. Biol. Chem.* **274,** 20049–20052
64. Carmody, R. J., and Cotter, T. G. (2001) *Redox Rep.* **6,** 77–90
65. Zhang, Z., Huang, C., Li, J., Leonard, S. S., Lanciotti, R., Butterworth, L., and Shi, X. (2001) *Arch. Biochem. Biophys.* **392,** 311–320
66. Bonny, C., Oberson, A., Negri, S., Sauser, C., and Schorderet, D. F. (2001) *Diabetes* **50,** 77–82
67. Ishiyama, S., Hiroe, M., Nishikawa, T., Shimojo, T., Abe, S., Fujisaki, H., Ito, H., Yamakawa, K., Kobayashi, N., Kasajima, T., and Marumo, F. (1998) *J. Immunol.* **161,** 4695–4701
68. Brunet, A., Bonni, A., Zigmond, M. J., Lin, M. Z., Juo, P., Hu, L. S., Anderson, M. J., Arden, K. C., Blenis, J., and Greenberg, M. E. (1999) *Cell* **96,** 857–868
69. Muzio, M., Chinnaiyan, A. M., Kischkel, F. C., O'Rourke, K., Shevchenko, A., Ni, J., Scaffidi, C., Bretz, J. D., Zhang, M., Gentz, R., Mann, M., Krammer, P. H., Peter, M. E., and Dixit, V. M. (1996) *Cell* **85,** 817–827
70. Kaufmann, S. H., and Hengartner, M. O. (2001) *Trends Cell Biol.* **11,** 526–534

71. Oberto, A., Marks, N., Evans, H. L., and Guidotti, A. (1996) *J. Pharmacol. Exp. Ther.* **279,** 435–442
72. Siegmund, D., Mauri, D., Peters, N., Juo, P., Thome, M., Reichwein, M., Blenis, J., Scheurich, P., Tschopp, J., and Wajant, H. (2001) *J. Biol. Chem.* **276,** 32585–32590
73. Chen, Y., and Lai, M. Z. (2001) *J. Biol. Chem.* **276,** 8350–8357
74. Chen, C. Y., Juo, P., Liou, J. S., Li, C. Q., Yu, Q., Blenis, J., and Faller, D. V. (2001) *Cell Growth Differ.* **12,** 297–306
75. Li, P., Nijhawan, D., Budihardjo, I., Srinivasula, S. M., Ahmad, M., Alnemri, E. S., and Wang, X. (1997) *Cell* **91,** 479–489
76. Chen, F., Demers, L. M., Vallyathan, V., Ding, M., Lu, Y., Castranova, V., and Shi, X. (1999) *J. Biol. Chem.* **274,** 20307–20312
77. Ye, J., Ding, M., Zhang, X., Rojanasakul, Y., Nedospasov, S., Vallyathan, V., Castranova, V., and Shi, X. (1999) *Mol. Cell. Biochem.* **198,** 193–200
78. Huang, C., Zhang, Z., Ding, M., Li, J., Ye, J., Leonard, S. S., Shen, H. M., Butterworth, L., Lu, Y., Costa, M., Rojanasakul, Y., Castranova, V., Vallyathan, V., and Shi, X. (2000) *J. Biol. Chem.* **275,** 32516–32522
79. Gao, N., Ding, M., Zheng, J. Z., Zhang, Z., Leonard, S. S., Liu, K. J., Shi, X., and Jiang, B. H. (2002) *J. Biol. Chem.* **277,** 31963–31971
80. Faris, M., Kokot, N., Latinis, K., Kasibhatla, S., Green, D. R., Koretzky, G. A., and Nel, A. (1998) *J. Immunol.* **160,** 134–144
81. Faris, M., Latinis, K. M., Kempiak, S. J., Koretzky, G. A., and Nel, A. (1998) *Mol. Cell. Biol.* **18,** 5414–5424
82. Kolbus, A., Herr, I., Schreiber, M., Debatin, K. M., Wagner, E. F., and Angel, P. (2000) *Mol. Cell. Biol.* **20,** 575–582
83. Aragane, Y., Kulms, D., Metze, D., Wilkes, G., Poppelmann, B., Luger, T. A., and Schwarz, T. (1998) *J. Cell Biol.* **140,** 171–182
84. Bennett, M., Macdonald, K., Chan, S. W., Luzio, J. P., Simari, R., and Weissberg, P. (1998) *Science* **282,** 290–293
85. Micheau, O., Solary, E, Hammann, A., and Dimanche-Boitrel, M. T. (1999) *J. Biol. Chem.* **274,** 7987–7992
86. Tang, D., Lahti, J. M., Grenet, J., and Kidd, V. J. (1999) *J. Biol. Chem.* **274,** 7245–7252
87. Bush, J. A., Cheung, K. J., Jr., and Li, G. (2001) *Exp. Cell Res.* **271,** 305–314
88. Tournier, C., Hess, P., Yang, D. D., Xu, J., Turner, T. K., Nimnual, A., Bar-Sagi, D., Jones, S. N., Flavell, R. A., and Davis, R. J. (2000) *Science* **288,** 870–874
89. Stennicke, H. R., Jurgensmeier, J. M., Shin, H., Deveraux, Q., Wolf, B. B., Yang, X., Zhou, Q., Ellerby, H. M., Ellerby, L. M., Bredesen, D., Green, D. R., Reed, J. C., Froelich, C. J., and Salvesen, G. S. (1998) *J. Biol. Chem.* **273,** 27084–27090
90. Scaffidi, C., Fulda, S., Srinivasan, A., Friesen, C., Li, F., Tomaselli, K. J., Debatin, K. M., Krammer, P. H., and Peter, M. E. (1998) *EMBO J.* **17,** 1675–1687
91. Kuida, K. (2000) *Int. J. Biochem. Cell Biol.* **32,** 121–124
92. D'Mello, S. R., Anelli, R., and Calissano, P. (1994) *Exp. Cell Res.* **211,** 332–338
93. Kunimoto, M. (1994) *Biochem. Biophys. Res. Commun.* **204,** 310–317